Research Paper

Volume : 3 | Issue : 11 | November 2014 • ISSN No 2277 - 8179

Structural and optical properties of Mn and Dy doped Zinc Aluminate nanoparticles

Physics

KEYWORDS : Sol gel, XRD, particle size, reflectance

K.Karunakaramoorthy Department of Engineering Physics, Faculty of Engineering and Technology, Annamalai University, Chidambaram-608002. Tamilnadu

G.Suresh Department of Engineering Physics, Faculty of Engineering and Technology, Annamalai University, Chidambaram-608002. Tamilnadu

ABSTRACT

The nanostructure of Zinc aluminate and doped Zinc aluminate were prepared by sol gel method using Zinc acetate, Aluminium acetate as starting material. Manganese acetate, dysprosium nitrate were used as dopent. The prepared samples were thermally annealed two hours at 900^{0}C. The annealed samples were characterized for their structural investigations using X-ray diffraction (XRD) analysis. Using the XRD data the average particle size was calculated by Scherrer equation and Williamson hall equation. The optical properties were determined by Diffuse Reflectance Spectroscopy (DRS). The results showed that the effect of Mn and Dy doping can affect the Crystallinity, particle size and optical properties of the Zinc aluminate nanoparticles.

Introduction:

Metal oxide nanostructured material has numerous potential applications in sensors, energy storing, photonics, electronics, optoelectronics, and harvesting device fabrications etc... Over the last few years, zinc oxide (ZnO) is a interesting II–VI compound semiconducting material, has attracted great attention due to its many remarkable properties with a large energy gap around Eg = 3.2 eV , large exciton binding energy (60 meV). Recently, a number of methods have focused on improving the ZnO properties by doping with metals and lanthanides [1, 2]. In general, there are several methods to synthesis the doped ZnO nano particle like solid-state reaction [3, 4], Combustion method [5], co-precipitation method [6], hydrothermal process [7], Pechini process [8] and sol–gel method [9]. The sol-gel methods have given numerous advantages such as a low temperature method, doping with other metals is straight forward, production of nanoparticals can be prepared easily and the structure of the product can be predetermined by varying the experimental conditions such as by the use of a capping agent or a change in pH and temperature.

In this paper, a sol–gel method was used to prepare Zinc aluminate, Mn doped Zinc aluminate and Dy doped Zinc aluminate nanoparticles. The influences of Mn and Dy doping on the Structural, particle size and optical properties of the Zinc aluminate particles were investigated by the X-ray diffraction (XRD) and diffuse reflectance spectroscopy (DRS).

Materials and Methods:

The procedure for the synthesis of Zinc aluminate, Mn and Dy doped Zinc aluminate nanoparticles are briefly summarized in Fig. 1.

The Zinc aluminates nanoparticles were prepared by sol gel method using Zinc acetate, aluminium acetate as a starting material. The manganese acetate, dysprosium nitrate were used as a doping material. 1M of Zinc acetate, aluminium acetate were dissolved in 2.methoxy ethanol.



Fig (1) Flow chart for the synthesis of Zinc aluminate, Mn and Dy doped Zinc aluminate nanoparticles

After 10 min magnetic stirring at room Temperature, the acidic acid and Ethylene glycol were added 1:1 ratio to the precursor solution. The acidic acid used as the gelling agent and Ethylene glycol act as reaction medium. The mixture was stirred 15 mints magnetically at room temperature. The pH of the resulting solution was adjusted at 10.3 using ammonium hydroxide. After completion of the reaction, The solution will keep under constant stirring at 80^{0}C temperature using magnetic stirrer for 1 hours and then dark brown color viscous sols was occurred. The resultant sol gels were dried for 5 hours at 80^0 C. The obtained powder was annealed at 900^{0}C for 2 hours. The similar process was repeated for the preparation of Mn and Dy doped Zinc aluminate nanoparticles by the respective stoichiometric amounts.

Result and discussion:

The crystalline phases and particle size of the obtained nanopowders were identified by X-ray diffraction (XRD) using a XPERT-PRO diffractometer. Fig 2(a-c) shows the XRD pattern of Zinc aluminate, Mn and Dy doped Zinc aluminate. All the diffraction peaks of Zinc aluminate, Mn and Dy doped Zinc aluminate samples could be fitted with the hexagonal wurtzite structure and all peak positions agree with the ZnO diffraction pattern (JCPDS-75-0576). There is no extra diffraction peak detected for Al, Mn and Dy. The results also indicate that the Mn and Dy ions systematically substituted for the Zn sites in the sample without changing the structure.

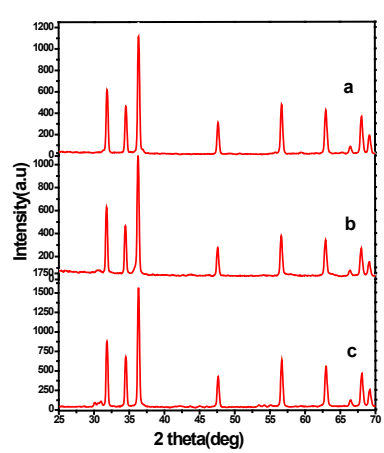

Fig2(a-c) XRD pattern of (a) Zinc Aluminate, (b) Mn doped Zinc

Aluminate, (c) Dy doped Zinc Aluminate samples annealed at 900^{0}c

The particle size has been carried out using the broadening of the XRD peaks. The importance of the broadening of peaks evidences grain modification along with the large strain associated with the Powder. The peak broadening of XRD analysis comes from different sources like instrument effect, finite crystallite size and strain effect within the crystal lattice [10]. Taking care of all the sources, particle size has been calculated using Scherrer's formula and Williamson- Hall plot method.

The instrumental broadening (βD) of the Zinc aluminate, Mn and Dy doped Zinc aluminate were corrected using the below relation and that is corresponding to each diffraction peak.

$$\beta_D^2=\beta_{measured}^2-\beta_{instrumental}^2 \text{ ----(1)}$$

The average particle sizes were estimated from the Scherrer's equation [11].

$$d=0.9\lambda/\beta\cos\theta_B \text{ ---------(2)}$$

Where λ is the x-ray wavelength of 1.54Å, θ_B is Bragg diffraction angle, and β is the FWHM of θ_B. The average particle sizes of the samples were calculated as 50.69, 68.50 and 68.23 nm, respectively. The Mn doped with Zinc aluminate increases the particle size and the Dy doped with Zinc aluminate decreases the particle size.

The particle size and strain broadening analysis was done Williamson and Hall method [12] depending on different θ positions. The strain induced broadening arising in the prepared powder due to crystal imperfections and distortion was calculated using below relation

$$\varepsilon=\beta_D/4\tan\theta\text{--------(3)}$$

The peak width from crystallite size varies as 1/cos θ and the strain varies as tan θ, it was confirmed from the above equation 2 and 3. The W-H method was derived based on the addition of Scherrer equation and strain results.

$$\beta=K\lambda/D\cos\theta+4\varepsilon\tan\theta\text{-----(4)}$$

Rearrange the above equation 4,

$$\beta\cos\theta=K\lambda/D+4\varepsilon\tan\theta\text{-----(5)}$$

The above equation is Williamson and Hall equation. The plots were drawn between 4tanθ along the X- axis and βcosθ along the Y-axis for as synthesized Zinc aluminate, Mn and Dy doped Zinc aluminate nanoparticles as shown in figure 3(a-c). After the linear fit to the data, the particle size was estimated from the Y-intercept and the Strain was calculated from the slop of the fit. The calculated average particle size , strain of the prepared nanopowders using W.H method and average particle size by Scherrer's method were shown in table (1).

Table.1. the average particle size (D) and strain (ε) of the synthesized nanoparticals using XRD

Sample	Particle size (nm)		Strain (10^{-4})
	Scherrer's Method	W.H method	
Al+ZnO	50.69	48.644	-0.6164
Al+Mn+ZnO	68.50	81.07	1.9165
Al+Dy+ZnO	68.23	88.30	2.8018

From the above table, the typical particle size values combuted from W-H method and scherrer's method. The particle size obtained using scherrer equation is smaller than that computed by W-H method. This is suitable to the fact that the scherrer equation does not take into account the effect of lattice strain and instrumental factors on peak broadening. This, in turn, expect too much of the effect of particle size on broadening of peaks and thus take too lightly particle size. From table (1) the negative value of the strain may be due to the lattice shrinkage that was observed in the calculation of lattice parameters

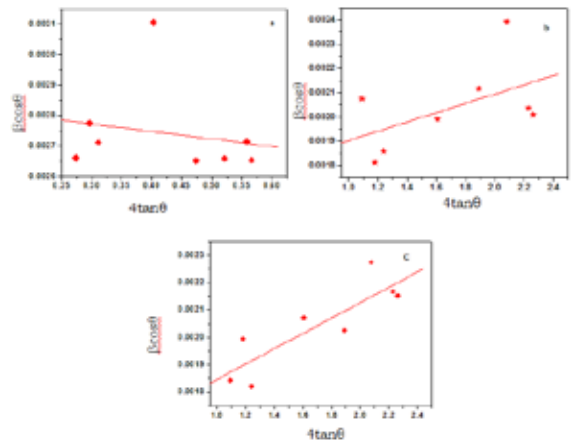

Fig.3(a-c) Williamson hall plot of (a) Zinc Aluminate,(b) Mn doped Zinc Aluminate,(c) Dy doped Zinc Aluminate samples annealed at 900^{0c}

The diffuse reflectance spectra of the Zinc Aluminate and Mn, Dy doped Zinc aluminate in the wavelength region (350nm-700nm) as shown in fig 4 (a-c). The reflectance of Zinc aluminate and Dy doped Zinc aluminate was 67% and 70% .The observed value of reflectance was decreased 22% for the Mn doped Zinc aluminate.

The reflectance spectrum of the Mn with Zinc aluminate can be attributed to the more prominent. The manganese doping in Zinc aluminate makes more defect sites as compared to Zinc aluminate and Dy doped Zinc aluminate [13]. When compared to the Zinc aluminate and Dy doped Zinc aluminate, the reflectance spectra of Mn doped Zinc aluminate is decreases due to the increase of the defect sites in the crystal structure. For analysis of diffuse reflectance (R) can be related to the Kubelka_Munk function F(R) by the relation $F(R) = (1-R)^2/2R$ [14].

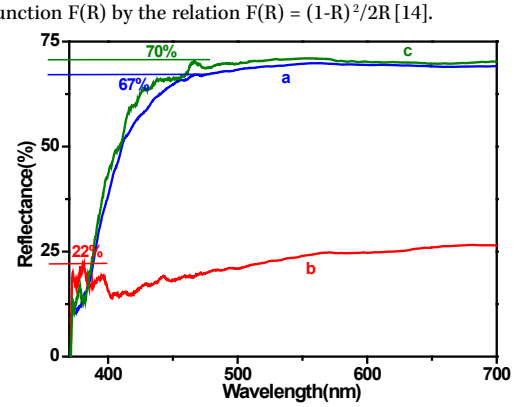

Fig.4 (a-c) The diffuse reflectance spectra of (a) Zinc Aluminate,(b) Mn doped Zinc Aluminate,(c) Dy doped Zinc Aluminate samples annealed at 900^{0}c

The band gap energy (E_g) for the Zinc Aluminate and Mn, Dy doped Zinc aluminate nanostructures were determined by the plot of the square of the modified Kubelka_Munk function vs. the photon energy (hν) [15], shown in Fig. 5(a-c). The band gap of the Zinc aluminate was 3.2451 eV, The Eg values of the Mn

Volume : 3 | Issue : 11 | November 2014 • ISSN No 2277 - 8179

and Dy doped Zinc aluminate samples are determined to be 3.1911 eV and 3.2353 eV.

In this work, the present study an attempt is made to correlate particle size with the band gap energy of the samples by varying the doping materials. The fig 6(a) shows the plot between the particle size Vs doping element.

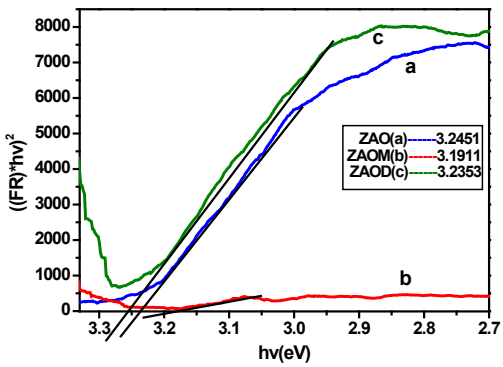

Fig.5(a-c) Plotting of ((FR)*hv)² versus the photon energy (hv) of (a) Zinc aluminate, (b) Mn doped Zinc aluminate, (c) Dy doped Zinc aluminate samples annealed at 900⁰c

The plot between band gap Vs doping element was investigated from fig (b). This difference could be caused by the different doping materials.

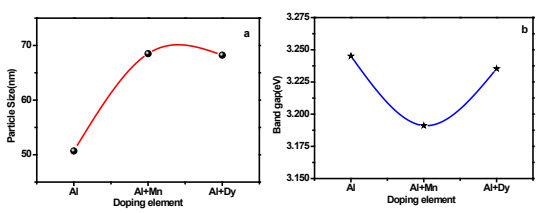

Fig.6The plots of (a) Particle size Vs doping element, (b) band gap Vs doping elements of Zinc Aluminate and Mn, Dy doped Zinc aluminate

The particle size of the Zinc aluminate was 50.69nm with the band gap 3.2451eV. After the Mn and Dy doped with Zinc aluminate, the particle size increases 68.51nm, 63.23nm and the band gap are decreases 3.1911eV, 3.2353eV.

Conclusion:

In this work, the Zinc aluminate, Mn and Dy doped Zinc aluminate were prepared by sol gel technique. The synthesized samples were characterized by XRD and Diffuse reflectance spectroscopy (DRS).The XRD analysis of Zinc aluminate and Mn, Dy doped Zinc aluminate were indicated that the nanoparticles have the hexagonal wurtzite structure. The average particle sizes of the samples were calculated as 50.69, 68.50 and 68.23 nm by scherrer method. Using W.H method the average sizes of the particle is 48.64, 81.07 and 88.30 nm. The connection between the structural and optical properties suggests that the particle sizes (50.69, 68.51 and 68.23 nm)of the samples are predominantly influenced the band gap energy of Zinc aluminate(3.2451eV) and Mn, Dy doped Zinc Aluminate(3.1911,3.2353 eV) nanoparticles.

REFERENCE

1.Mu-Tsun Tsai, Yu-Xiang Chen, Pei-Jane Tsai, Yen-Kai Wang, Photoluminescence of Manganese-doped ZnAl2O4 nanophosphors, Thin Solid Films, 518 (2010) e9–e11, | 2. Yongsheng Liu,Renfu Li,Wenqin Luo, Haomiao Zhu,and Xueyuan Chen, Optical Spectroscopy of Sm3+ and Dy3+ Doped ZnO Nanocrystals, Spectroscopy Letters, 43 (2010) 343–349. | 3. W.-S. Hong, L.C. De Jonghe, X. Yang, M.N. Rahaman, Reaction sintering of ZnO–Al2O3, J. Am. Ceram. Soc. 78 (1995) 3217–3224. | 4. N.J. van der Laag, M.D. Snel, P.C.M.M. Magusin, G. de With, Structural, elastic, thermo physical and dielectric properties of zinc aluminate, J. Eur. Ceram. Soc, 24 (2004) 2417–2424. | 5. A.K. Adak, A. Pathak, P. Pramanik, Characterization of ZnAl2O4 nanocrystals prepared by the polyvinyl alcohol evaporation route, J.Mater. Sci. Lett. 17 (1998) 559–561. | 6. M.A. Valenzuela, J.P. Jacobs, P. Bosch, S. Reijne, B. Zapata, H.H. Brongersma, The influence of the preparation method on the surface structure of ZnAl2O4, Appl.Catal. A: Gen 148 (1997) 315–324. | 7. H. Grabowska, W. Mista, J. Trawczyski, J. Wrzyszcz, M. Zawadzki, A method for obtaining thymol by gas phase catalytic alkylation of m-cresol over zinc aluminate spinel, Appl. Catal. A: Gen. 220 (2001) 207–213. | 8. H. Serier, M. Gaudon, M. Ménétrier, Al-doped ZnO powdered materials: Al solubility limit and IR absorption properties, | Solid State Sciences, 11 (2009) 1192–1197. | 9. A. Louiza, H. Saliha, H. Sofiane, G. Kamel, G. Lakhder, Structural and luminescence properties of pure and Al-doped ZnO nanopowders, Mater. Sci. Eng., B 177 (2012) 902–907. | 10. C Suryanarayana,, MG Nortan,: X-ray diffraction: a practical approach. Plenum Publishing Corporation, New York (1998) | 11. B.D. Cullity, Elements of X-Ray Diffraction, Addison-Wesley, Reading, MA, 1978. 102. | 12. G. K. Williamson, W. H. Hall: X-ray line broadening from filed Aluminium and Wolfram, Acta Metall., 1 (1953) 22. | 13. Ruh Ullah, Joydeep Dutta, Photocatalytic degradation of organic dyes with manganese-doped ZnO nanoparticles, Journal of Hazardous Materials 156 (2008) 194–200. | 14. Kortum, G. Reflectance Spectroscopy; Springer – Verlog: New York (1969). | 15. Cao, G., Rabenberg, L. K., Nunn, C. M, Mallouk, T.E. Formation of Quantum-Size Semiconductor Particles in a Layered Metal Phosphonate Host Lattice, Chem. Matter, 3 (1991) 149-156. |